Modern Physics Letters B
Vol. 31, No. 31 (2017) 1750291 (15 pages)

DOI: 10.1142/S0217984917502918

Evolvement law of a macroscopic traffic model accounting for density-dependent relaxation time

Yu-Qing Wang[*,†,§], Xing-Jian Chu[‡], Chao-Fan Zhou[‡], Bin Jia[†,¶],
Sen Lin[‡], Zi-Han Wu[‡], Hua-Bing Zhu[*,‖] and Zi-You Gao[†]

[*] *School of Mechanical Engineering,
Hefei University of Technology, Hefei 230009, China*
[†] *MOE Key Laboratory for Urban Transportation Complex Systems Theory and Technology,
Beijing Jiaotong University, Beijing 100044, China*
[‡] *School of Physical Sciences, University of Science and Technology of China,
Hefei 230026, China*
[§] *yuqingw@mail.ustc.edu.cn*
[¶] *bjia@bjtu.edu.cn*
[‖] *hfuthbzhu@163.com*

Received 25 June 2017
Revised 15 July 2017
Accepted 18 July 2017
Published 4 September 2017

In this paper, a modified macroscopic traffic flow model is presented. The term of the density-dependent relaxation time is introduced here. The relation between the relaxation time and the density in traffic flow is presented quantitatively. Besides, a factor R depicting varied properties of traffic flow in different traffic states is also introduced in the formulation of the model. Furthermore, the evolvement law of traffic flow with distinctly initial density distribution and boundary perturbations is emphasized.

Keywords: Macroscopic traffic flow model; relaxation time; evolvement law.

1. Introduction

With the rapid development of road traffic, tremendous problems (e.g. congestion,[1–5] traffic bottlenecks,[6–10] volatile organic compounds emissions[11–16]) have been brought out. In order to well illustrate the real traffic, numerous models have been put forward within several decades. Generally speaking, mainstream models can be divided into three kinds (e.g. macroscopic models,[10] microscopic ones[17–19] and mesoscopic ones[20]). Several outstanding models have been presented. For instance, LWR model[21] is one of the most famous models in modeling traffic flow in

[§,¶,‖]Corresponding authors.

the macroscopic view. Open boundary conditions and the continuity equation were introduced to get the density function. Besides, motivated by LWR, PW model[22] was proposed, where dynamic equations were first introduced to simulate the real traffic. Moreover, KK model[23] developed the macroscopic one, where the speed–density function composed by the free velocity and the jam density was considered. Furthermore, Tang focused on tremendous microscopic traffic flow models such as considering the traffic interruption probability,[24] the micro driving behavior,[25] the effect of signal lights on the fuel consumption,[26] MVFS,[27] NVFS[28] in the car-following model and so on. Finally, Xiao[29–34] and Wang[35–39] applied traffic flow models into the mesoscopic view.

The evolvement of car-following models illustrating the real traffic is one of the most important issues in the research of traffic flow. Pipes first raised the car-following model considering the impact of headway on drivers' sensitivities.[40] Since then, a series of modifications were made under the enlightening research. Nagatani promoted the model by studying the phase transition of traffic flow among the freely-moving phase, the coexisting one and the uniform-congested one.[41] Afterwards, Jiang proposed the velocity gradient model.[42] The model took it into consideration that when the velocity of the previous vehicle was high, the instantaneous headway could be shorter than the safe headway. On the basis of the former studies, Bando[43] presented OV model by introducing optimal velocity that depends on the following distance of the preceding vehicle.

However, few models concentrate on the effect of traffic states on traffic flow. Treiber proposed GKT model[44] in order to study traffic flow on different streets that are homogeneous inside. Jiang[45] carried out car-following simulations on a circle road and pointed out that car-following process would cause fluctuations in spacing. Nevertheless, varied traffic states and corresponding impacts were not taken into account in their work. Recently, Tang[46] raised a macroscopic traffic flow model accounting for real-time traffic state. The influence of traffic states on traffic flow was calculated. The relaxation time remained constant, however, in the real world, it does have connections with the density in traffic flow. Under different circumstances of traffic states, different drivers will have varied reactions. Generally, the higher the density is, the shorter the relaxation time becomes. Motivated by this fact, this paper not only considers the effect of traffic states on traffic flow, but also treats the relaxation time as a density-dependent variable. Besides, the impact of the relaxation time on the evolvement of traffic flow is addressed.

The organization of the paper is given as follows. In Sec. 2, a modified macroscopic traffic flow model is introduced to illustrate the traffic flow in an open-boundary road section. Besides, experiments about the traffic state factor R are performed in Sec. 3. Moreover, the evolvement of traffic flow is emphasized with the consideration of varied initial global density ρ_0. Furthermore, effects of characteristic parameters (e.g. the density ρ, the velocity v, the flow J and deviations of velocities v_D) are calculated. All in all, conclusions are summarized in Sec. 4.

Name	Physical Meaning	Unit
x	Spatial variable	m
t	Time variable	s
ρ	Traffic density	veh/m
ρ_{max}	The jam density	veh/m
v	Speed	m/s
v_r	Speed adjustment term	m/s
v_f	Free flow speed	m/s
$v_e(\rho)$	Equilibrium speed without road condition	m/s
$v_{r,e}(\rho)$	Equilibrium speed with road condition	m/s
τ	Relaxation time	s
$c_{r,0}$	Propagation speed of small perturbation under road condition	m/s
a_r	Acceleration adjustment term	m/s^2

Fig. 1. Parameters denoted in the proposed model.

2. Model

In this section, a macroscopic traffic model accounting for the density-dependent relaxation time is proposed. Different with Tang's work,[46] control equations of the system can be expressed as

$$\begin{cases} \rho_t + (\rho v)_x = 0, \\ v_t + v v_x = \dfrac{v_{r,e}(\rho) - v}{\tau} + c_{r,0} v_x + \eta_r (R(x+\Delta x) - R(x)) a_r, \\ v_{r,e}(\rho(x,t)) = v_e(\rho(x,t)) + \eta_r (R(x+\Delta x) - R(x)) v_r, \\ v_e = v_f \left(\left(1 + \exp\left(\dfrac{\rho/\rho_{\max} - 0.25}{0.06} \right) \right)^{-1} - 3.72 \times 10^{-6} \right), \\ \tau = 150 \exp\left(\dfrac{1}{\rho - \rho_c} \right). \end{cases} \tag{1}$$

Here, tremendous parameters are introduced in the model formulation, which can be found in Fig. 1. Besides, $\rho_{\max}$ represents the congestion density which is the critical point of phase transitions. Moreover, ρ_c represents the critical point where the value of the relaxation time becomes zero. Furthermore, both of these parameters are of relatively high density. However, the value of ρ_c is slightly higher than that of $\rho_{\max}$, since the relaxation time corresponding to the congestion state is not always zero.

The first expression in Eq. (1) is the continuity equation. Here, η_r is a parameter reflecting the influence of traffic state on traffic flow. It is an empirical parameter which depends on density of traffic flow. According to the numerical results, η_r has no effect on traffic flow when density is very low or high. It works when the density is moderate.

The second one corresponds to non-equilibrium properties of traffic flow. Besides, in order to avoid the wrong-way travel problem, the term $c_{r,0}v_x$ is introduced, which can reflect realistic driving behaviors. In details, $c_{r,0}v_x$ considers the acceleration effect caused by the relative speed. Meanwhile, it can eliminate the phenomenon of backward movement. Moreover, similar to Ref. 46, the parameter $R(x)$ is introduced to depict traffic states of real traffic, which depends on densities in traffic flow, the system size and road qualities (e.g. the roughness, pavement materials, etc.). Furthermore, the value of $R(x)$ is in the interval $[-1, 1]$. Here, $R(x)$ works with η_r and the acceleration adjustment term a_r to influence the variation of velocity. Therefore, $R(x)$ has a relative value. Theoretically, its value can be set in any range. However, in order to illustrate the traffic state in a simple way, we choose the interval $[-1, 1]$. Then, the value of η_r and a_r can be determined. The relationship between the specific value of $R(x)$ and the traffic state can be summarized as follows:

$$\begin{cases} \text{light} & R(x) > 0\,, \\ \text{medium} & R(x) = 0\,, \\ \text{heavy} & R(x) < 0\,. \end{cases} \tag{2}$$

In details, $R(x) > 0$ means that the traffic is light, while $R(x) < 0$ corresponds to the heavy traffic. Besides, $R(x) = 0$ reflects the medium case.

However, the third expression in Eq. (1) depicts the equilibrium velocity under specific road conditions. The equilibrium speed $v_{r,e}$ under road conditions is modified with the traffic state factor $R(x)$, which considers that the acceleration is caused by relative conditions of a section. Besides, in fact, the equilibrium speed with road condition is derived under the circumstances that traffic flow has reached the equilibrium state. Thus, the equation $v_t = v_x = 0$ is satisfied. Moreover, by means of substituting it into the second formula of Eq. (1), we can get $v_{r,e}(\rho(x,t)) = v_e(\rho(x,t)) + \eta_r(R(x+\Delta x, t) - R(x,t))a_r\tau$. Thus, by setting $v_r = a_r\tau$ as the speed adjustment term, we can get the third formula in Eq. (1).

Moreover, similar to Ref. 46, the relationship between the equilibrium speed v_e and the free flow speed v_f can be expressed as the fourth one in Eq. (1). Actually, the forth expression is used to illustrate the equilibrium speed v_e. It was first derived in Ref. 47. Then, Kerner applied it to his macroscopic traffic flow model on the basis of Navier–Stokes equation.[23] Besides, coefficients in the fourth expression in Eq. (1) were obtained and modified by the empirical data in order to illustrate the traffic wave dynamics.

Furthermore, the fifth expression in Eq. (1) is obtained from the following facts. On one hand, the greater the density is, the shorter the relaxation time becomes. Because when the headway is short, the velocity is relatively small and the driver's sensitivity is relatively high, which leads vehicles to sooner recovering to the equilibrium positions, respectively, after adding a slight disturbance. On the other hand, the lower the density is, the longer the relaxation time becomes. Because the following driver needs longer time to react when the minor disturbance causes the

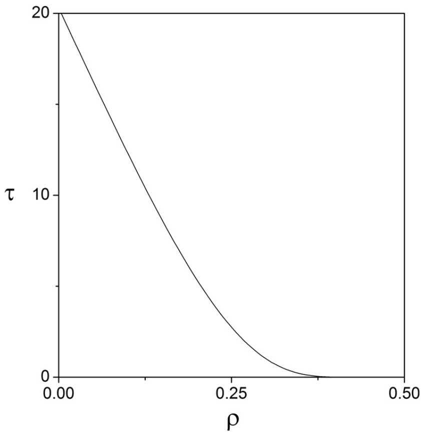

Fig. 2. The relationship between the relaxation time and the density.

previous driver's speed to change and the headway is long. Besides, a longer acceleration or deceleration time is required when the speed is higher. Here, ρ_c represents the critical density of traffic jam. Moreover, the relaxation time obeys the fifth expression in Eq. (1), when $\rho < \rho_c$ is satisfied. Furthermore, the relaxation time becomes 0, when $\rho > \rho_c$ is satisfied. Finally, Fig. 2 shows the relationship between τ and ρ.

3. Numerical Simulation Experiments

In this part, we study the evolution of traffic flow on an open-boundary section with perturbations. Two cases are presented here. The first one is introducing a cosine function to denote $R(x)$. The other one is using pseudo-random sequences to illustrate $R(x)$. First of all, the difference method is applied into the analysis of Eq. (1). The following equation can be obtained:

$$\rho_i^j = \rho_i^{j-1} + \frac{\Delta t}{\Delta x}\rho_i^{j-1}(v_{i+1}^{j-1} - v_i^{j-1}) + \frac{\Delta t}{\Delta x}v_i^{j-1}(\rho_i^{j-1} - \rho_{i-1}^{j-1})\,. \tag{3}$$

In details, Eq. (3) is derived from the first expression in Eq. (1). According to Ref. 42, the upwind difference scheme can well describe the traffic wave. Thus, the upwind difference scheme is applied to Eq. (1), which leads to equation $\frac{1}{\Delta t}(\rho_i^j - \rho_i^{j-1}) = \frac{1}{\Delta x}[\rho_i^{j-1}(v_i^{j-1} - v_{i+1}^{j-1}) + v_i^{j-1}(\rho_{i-1}^{j-1} - \rho_i^{j-1})]$. Thus, by means of rewriting the formula into the recursive form, we can obtain Eq. (3). In the process of the discretization, the non-equilibrium equation of velocity should be treated differently under various circumstances.

On one hand, when the traffic is heavy (namely, $v_i^{j-1} < c_{r,0}$), the variation of velocity is mainly affected by the velocity difference between the ith vehicle and the previous one (namely, the $(i+1)$th vehicle). Thus, the discrete format of the non-equilibrium equation of velocity can be written as

$$v_i^j = v_i^{j-1} + \frac{\Delta t}{\Delta x}(c_{r,0} - v_i^{j-1})(v_{i+1}^{j-1} - v_i^{j-1}) + \frac{\Delta t}{150} e^{-\frac{1}{\rho_i^j - \rho_c}} (v_{r,e}(\rho_i^{j-1}) - v_i^{j-1}) + \Delta t \eta_r (R(i+1, j-1) - R(i, j-1)) a_r \,. \quad (4)$$

On the other hand, when the traffic is light (namely, $v_i^{j-1} > c_{r,0}$), the variation of velocity is mainly affected by the difference of velocity between the ith vehicle and the following one (namely, the $(i-1)$th vehicle). Similarly, the discrete format can be obtained as follows:

$$v_i^j = v_i^{j-1} + \frac{\Delta t}{\Delta x}(c_{r,0} - v_i^{j-1})(v_i^{j-1} - v_{i-1}^{j-1}) + \frac{\Delta t}{150} e^{-\frac{1}{\rho_i^j - \rho_c}} (v_{r,e}(\rho_i^{j-1}) - v_i^{j-1}) + \Delta t \eta_r (R(i+1, j-1) - R(i, j-1)) a_r \,. \quad (5)$$

Here, i, j, Δx, Δt represent the space index, the time index, the space-step length and the time-step length, respectively.

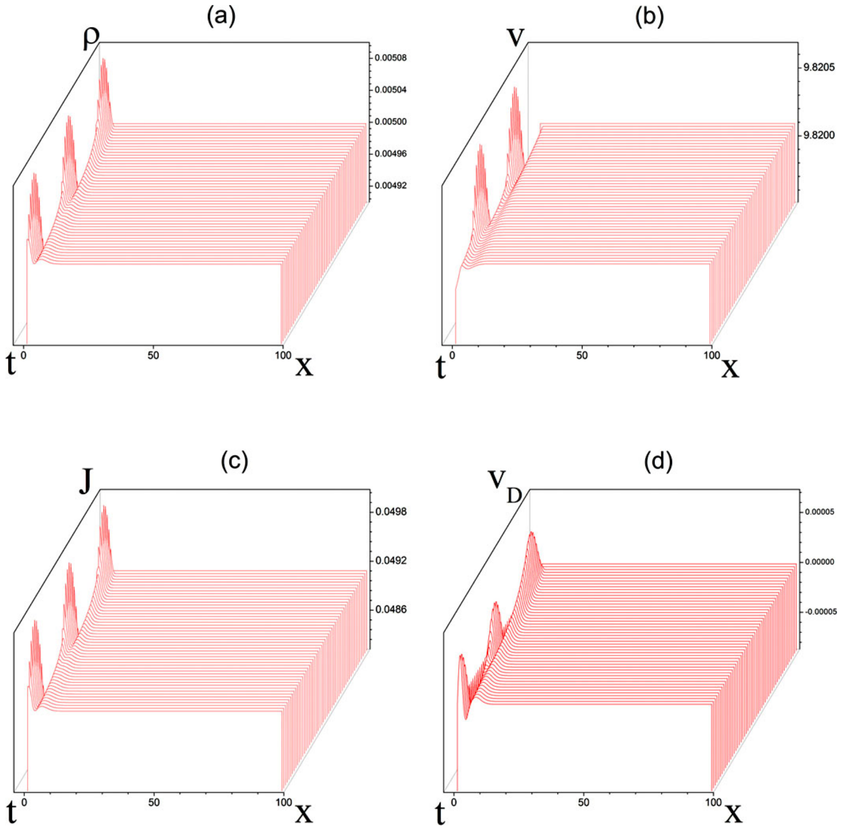

Fig. 3. The evolvement of traffic flow under the condition that $R(x) = \cos(\frac{\pi x}{15})$ is satisfied. The simulation time t satisfies $t = 50$ s. (a) the density in the section; (b) the velocity; (c) the current; (d) the deviation of the velocity. Here, the low density case is considered. Besides, $\rho_0 = 0.005$.

For simplicity, we assume the initial density ρ_0 as a fixed value and the initial velocity of traffic flow as the equilibrium speed $v_{r,e}(\rho)$. Besides, a minor perturbation $\rho_{bd}(0,t)$ is introduced as the left-boundary condition, which can be expressed as follows:

$$\rho_{bd}(0,t) = \rho_0 \left[1 + 0.02 \sin\left(\frac{\pi t}{10}\right)\right]. \tag{6}$$

Moreover, specific values of corresponding parameters are set as follows:

$$c_{r,0} = \begin{cases} 8, & R(x+\Delta x) - R(x) > 0\,, \\ 5, & R(x+\Delta x) - R(x) = 0\,, \\ 4, & R(x+\Delta x) - R(x) < 0\,, \end{cases} \tag{7}$$

$$\eta_r = \begin{cases} 0, & \text{if } \rho > 0.05 \quad \text{or} \quad \rho < 0.01\,, \\ 0.5, & \text{otherwise,} \end{cases} \tag{8}$$

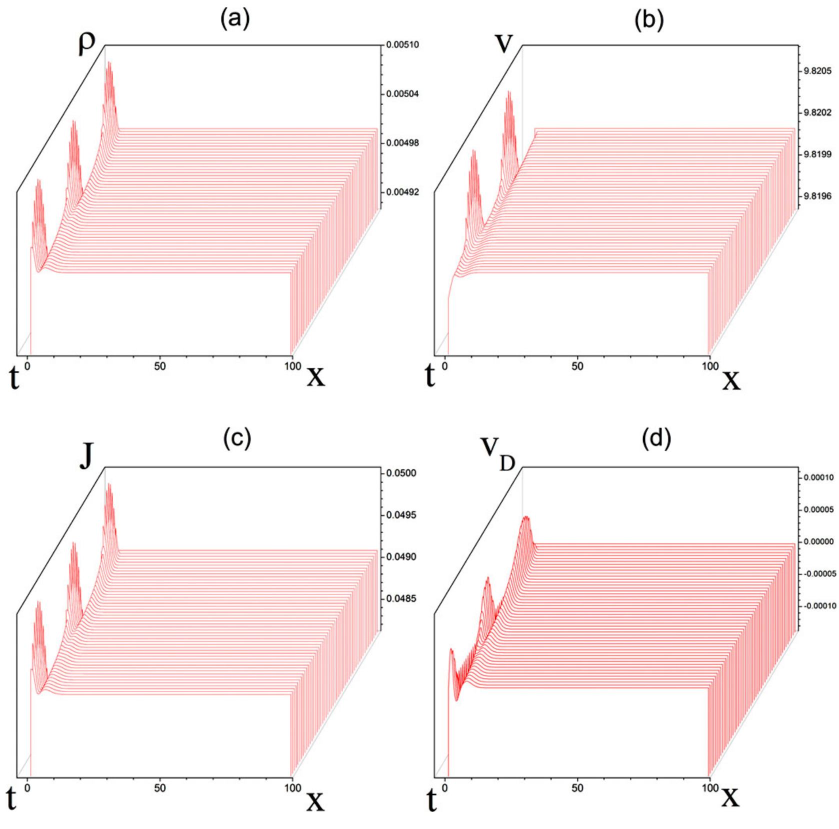

Fig. 4. The evolvement of traffic flow under the condition that pseudo-random sequences in the interval $[-1, 1]$ are chosen as $R(x)$. The simulation time t satisfies $t = 50$ s. (a) the density in the section; (b) the velocity; (c) the current; (d) the deviation of the velocity. Here, the low density case is considered. Besides, $\rho_0 = 0.005$.

$$a_r = \begin{cases} 0, & \text{if } \rho > 0.05 \quad \text{or} \quad \rho < 0.01\,, \\ 0.5, & \text{otherwise,} \end{cases} \tag{9}$$

and

$$v_r = \begin{cases} 0, & \text{if } \rho > 0.05 \quad \text{or} \quad \rho < 0.01\,, \\ 2, & \text{otherwise.} \end{cases} \tag{10}$$

Furthermore, $v_f = 10$ m/s, $\rho_c = 0.5$ veh/m, $\Delta x = 100$ m, $\Delta t = 1$ s and the number of space steps $N = 100$ are calculated. Thus, the system size satisfies $L = 10$ km.

Then, four situations are investigated in this part. First, the low density situation is calculated, where $\rho_0 = 0.005$ veh/m is satisfied. Besides, two cases are considered. On one hand, results of $R(x) = \cos(\frac{\pi x}{15})$ are presented in Fig. 3. The evolvement of the density, velocity, flow and deviation of velocities is displayed in Figs. 3(a)–3(d), respectively. On the other hand, pseudo-random sequences in the

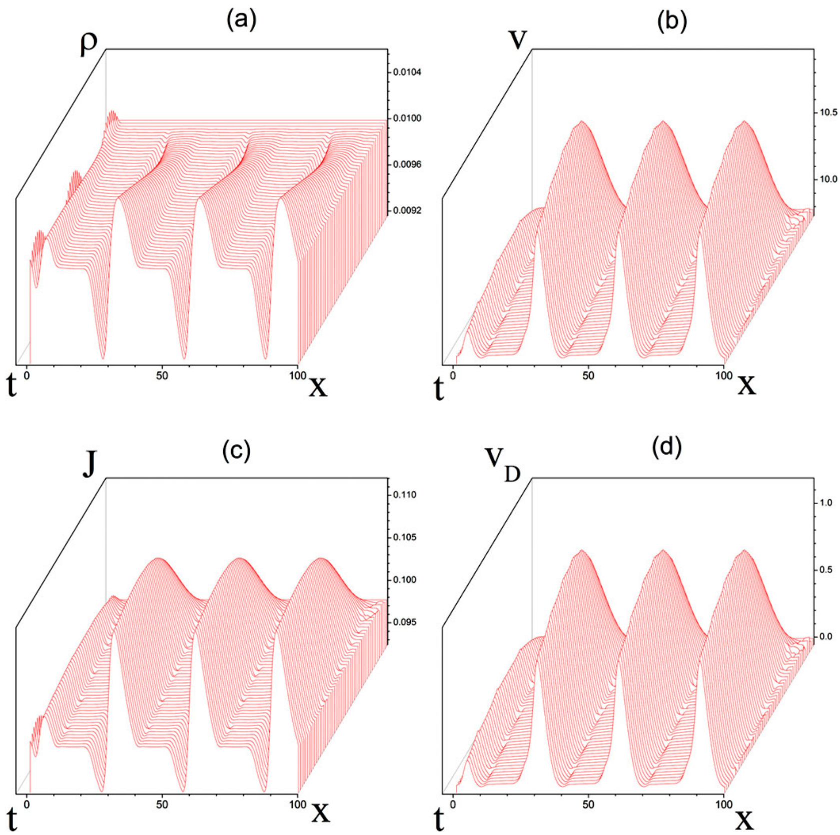

Fig. 5. The evolvement of traffic flow under the condition that $R(x) = \cos(\frac{\pi x}{15})$ is satisfied. The simulation time t satisfies $t = 50$ s. (a) the density in the section; (b) the velocity; (c) the current; (d) the deviation of the velocity. Here, the relatively low density case is considered. Besides, $\rho_0 = 0.01$.

interval $[-1, 1]$ are chosen as the format of $R(x)$. Similar results are displayed in Fig. 4. From Figs. 3 and 4, it can be found that traffic flow can soon be stable, when the density in the system is low. Besides, when the balance is reached, the density, flow and deviation of the velocity are small, while the velocity is quite high. Such phenomenon indicates that the traffic state factor $R(x)$ has little impact on the evolution of traffic flow when the density is very low. In another view, the low density leads to the huge headway. Thus, minor perturbations have little impact on the following vehicle and will soon dissipate. Besides, although two different formats of $R(x)$ are applied in this situation, similar results can be obtained. Thus, the initial density dominates the evolvement of traffic flow in this case.

Second, the relatively low density situation is calculated, where $\rho_0 = 0.01$ veh/m is satisfied. Similar to the above situation, $R(x) = \cos(\frac{\pi x}{15})$ and pseudo-random sequences are also applied here. Figures 5 and 6 display the corresponding results. From Fig. 5, it can be found that there are four states of densities, namely, the

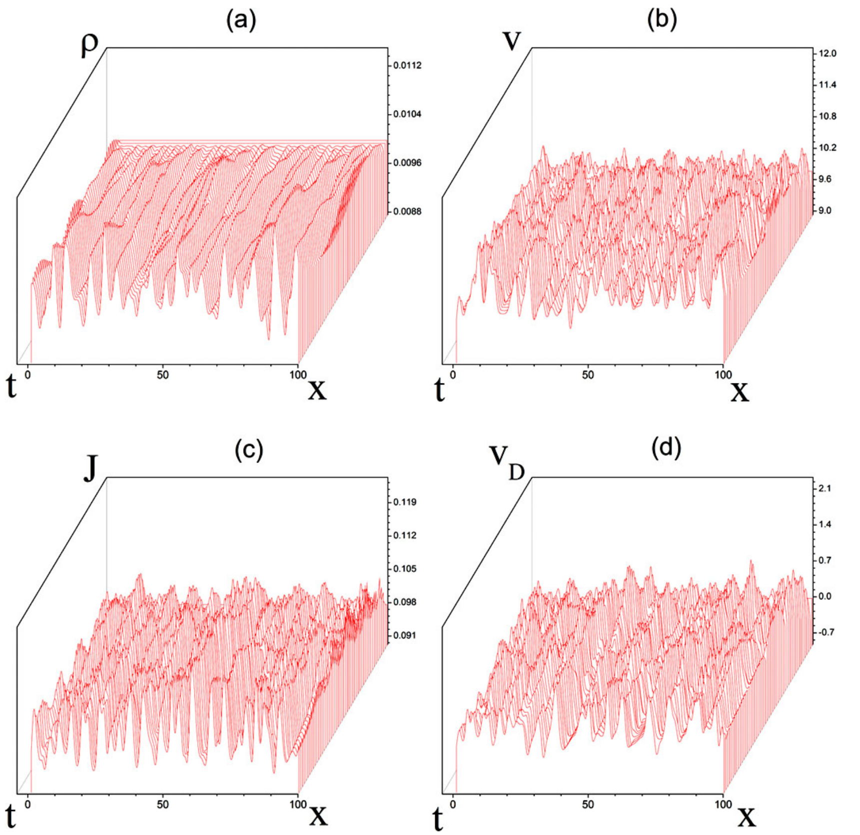

Fig. 6. The evolvement of traffic flow under the condition that pseudo-random sequences in the interval $[-1, 1]$ are chosen as $R(x)$. The simulation time t satisfies $t = 50$ s. (a) the density in the section; (b) the velocity; (c) the current; (d) the deviation of the velocity. Here, the relatively low density case is considered. Besides, $\rho_0 = 0.01$.

increasing part, the shrinking one, the flat one and the second shrinking one. It can be explained by real traffic. In details, when vehicles encounter heavy traffic, the traffic capacity shrinks and increasing densities emerge. Then, velocities of vehicles tend to be in equilibrium and the headway tends to be unvaried, which contributes to densities declining and maintaining unchanged then. Afterwards, since the total number of vehicles is conserved, there will be a state where the density is very low and the speed is relatively high. From Fig. 6, it can be concluded that the traffic state factor has a great influence on the evolution of traffic flow in this situation. In other words, when $R(x)$ is a random digit, the evolvement of the density wave and the velocity wave is accordingly irregular.

Third, the relatively high density situation is considered, where $\rho_0 = 0.03$ veh/m is satisfied. Similar to above situations, two formats of $R(x)$ are also applied here. Figures 7 and 8 show the corresponding results. From Fig. 7, it can be found that

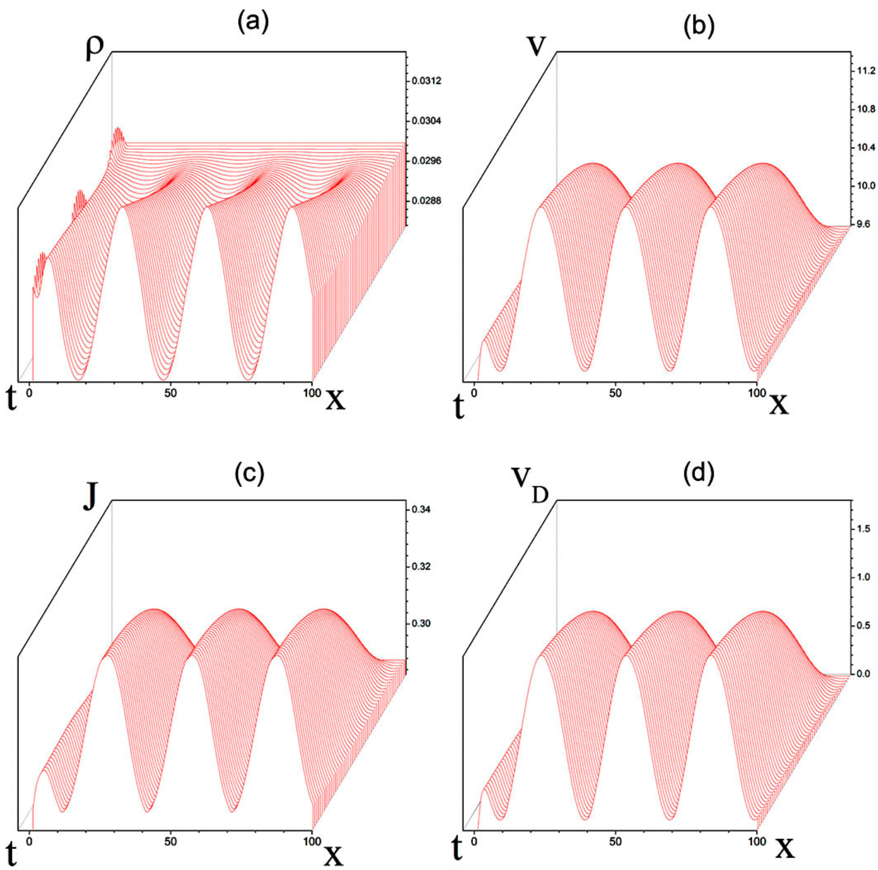

Fig. 7. The evolvement of traffic flow under the condition that $R(x) = \cos(\frac{\pi x}{15})$ is satisfied. The simulation time t satisfies $t = 50$ s. (a) the density in the section; (b) the velocity; (c) the current; (d) the deviation of the velocity. Here, the relatively high density case is considered. Besides, $\rho_0 = 0.03$.

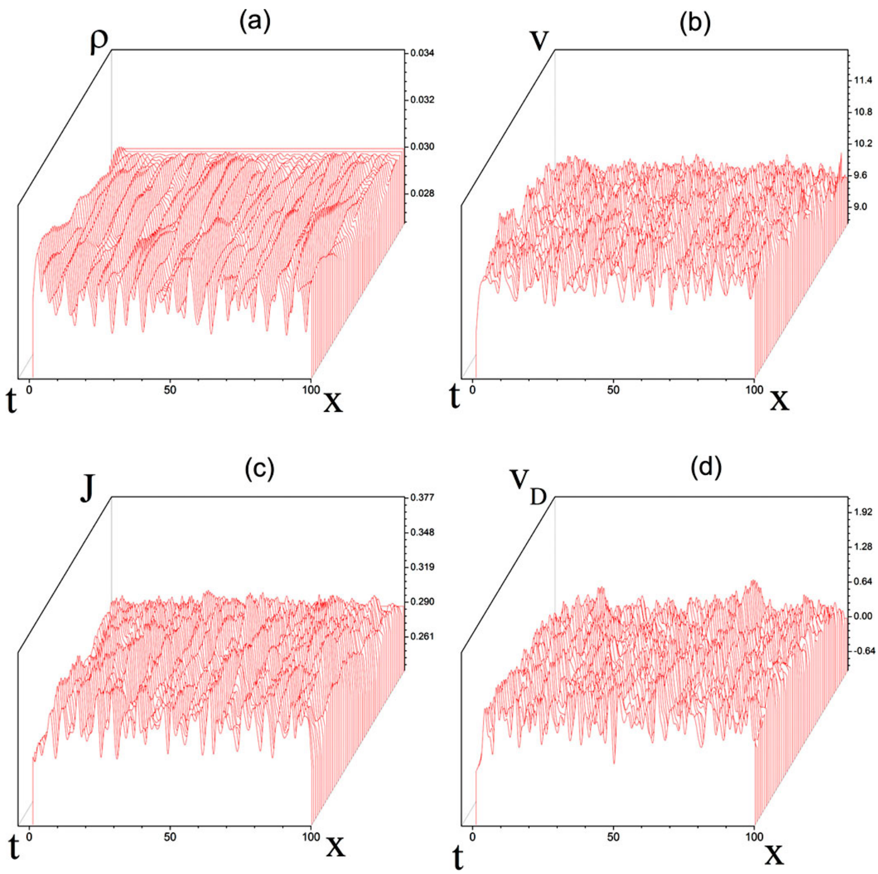

Fig. 8. The evolvement of traffic flow under the condition that pseudo-random sequences in the interval $[-1, 1]$ are chosen as $R(x)$. The simulation time t satisfies $t = 50$ s. (a) the density in the section; (b) the velocity; (c) the current; (d) the deviation of the velocity. Here, the relatively high density case is considered. Besides, $\rho_0 = 0.03$.

the flat state of the density disappears. Compared with Fig. 5, Fig. 7 shows that the flat state gradually shrinks with an increase of the density under the condition $R(x) = \cos(\frac{\pi x}{15})$. Integrated with the reality, the flat state means the achievement of balanced traffic flow. However, when the density is relatively high, vehicles come to the next traffic bottleneck before they make it to the equilibrium state. Meanwhile, similar to Fig. 6, Fig. 8 shows that the traffic state factor also has a great impact on the evolution of traffic flow in this situation. Similarly, when $R(x)$ is a random digit, the evolvement of the density wave and the velocity wave is accordingly irregular.

Finally, the high density situation is calculated, where $\rho_0 = 0.3$ veh/m is satisfied. Similar to the above situations, two formats of $R(x)$ are also applied here. Figures 9 and 10 show the corresponding results. Actually, results obtained in this situation are similar to those in the low density one. When the balance is reached,

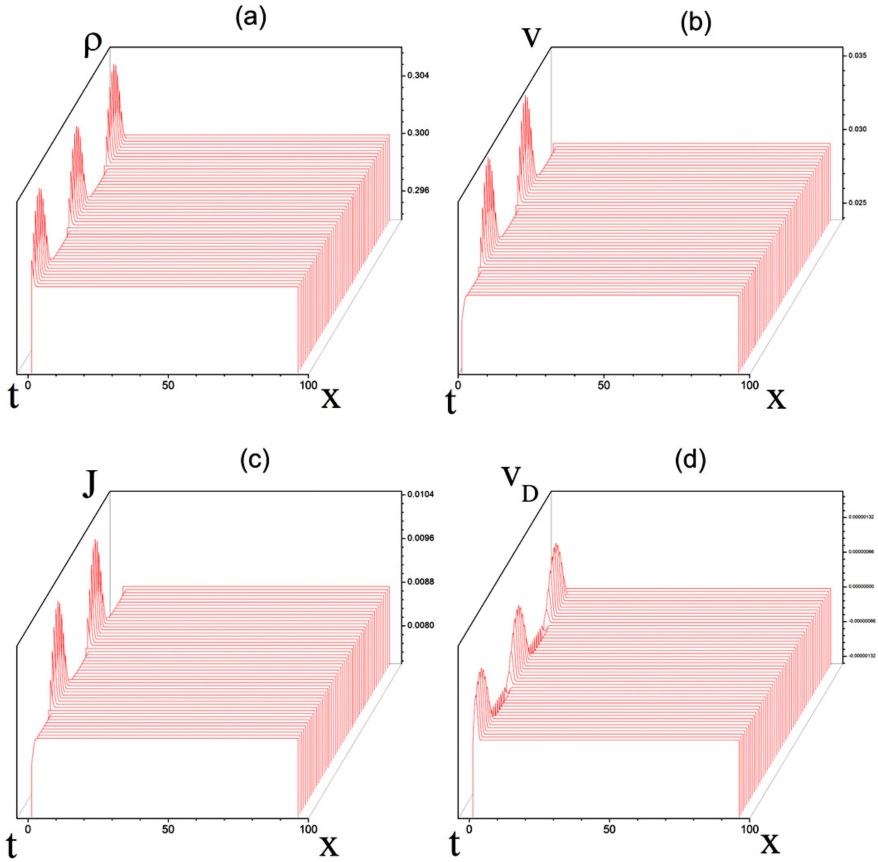

Fig. 9. The evolvement of traffic flow under the condition that $R(x) = \cos(\frac{\pi x}{15})$ is satisfied. The simulation time t satisfies $t = 50$ s. (a) the density in the section; (b) the velocity; (c) the current; (d) the deviation of the velocity. Here, the high density case is considered. Besides, $\rho_0 = 0.3$.

the density is high while both the velocity and the flow are rather low. Similar to the low density situation, the traffic state factor $R(x)$ has little effect on the evolution of traffic flow. In another view, the velocity is generally low and the relaxation time is short, when the density is high. Besides, comparing Figs. 9 and 10, it can be concluded that perturbations have little impact on the following vehicle and they will soon be suppressed. Thus, in the high density situation, the relaxation time dominates in the evolvement of traffic flow. Here, the deviation of the velocity of traffic flow represents the difference between the real-time velocity and the equilibrium velocity. Figures depicting the deviation can reflect whether the traffic flow has reached the equilibrium and the extent to which the state of traffic flow deviates from the equilibrium. With the help of (d) in Figs. 3–10, we can draw the conclusion that perturbations from the left boundary have no impacts on traffic flow when the density is very low or high, while they work when the density is moderate.

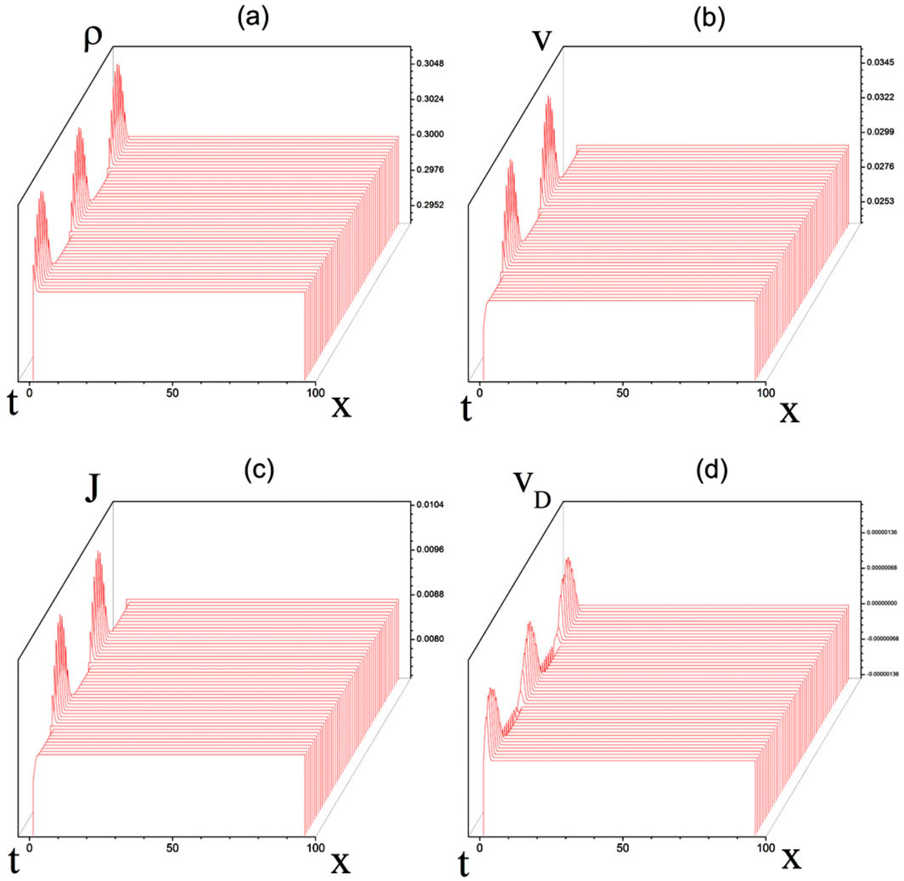

Fig. 10. The evolvement of traffic flow under the condition that pseudo-random sequences in the interval $[-1, 1]$ are chosen as $R(x)$. The simulation time t satisfies $t = 50$ s. (a) the density in the section; (b) the velocity; (c) the current; (d) the deviation of the velocity. Here, the high density case is considered. Besides, $\rho_0 = 0.3$.

4. Conclusion

In this paper, a modified macroscopic traffic flow model coupled with the density-dependent relaxation time accounting for the traffic state is proposed. The impacts of the specific road condition factor $R(x)$ on the evolvement of traffic flow are emphasized. Detailed illustrations of the transfer and dissipations of the perturbation in traffic flow are presented. Moreover, numerical simulation experiments of a settled open-boundary section are intensively performed and four different situations (namely, the low density condition, the relatively low one, the relatively high one and the high density one) are discussed. Furthermore, applications of the model into a circular road will be discussed in our intending paper.

Acknowledgments

Dr. Yu-Qing Wang would like to thank the Fundamental Research Funds for the Central Universities (JZ2015HGBZ0465), the China Postdoctoral Science Foundation (2016M590041), the Fund of Ministry of Labour and Social Security of the People's Republic of China (No. 102-411209), the Research Fund of Department of Environmental Protection of Anhui Province in China (JZ2016AHST1098) and the Enterprise Research Project (W2016JSKF0252). Prof. Bin Jia and Prof. Zi-You Gao thank the NNSFC support (Nos. 71621001, 71631002, 71471012 and 71222101) and the National Basic Research Program of China (No. 2012CB725404). Noted that Yu-Qing Wang and Xing-Jian Chu made equal contributions to the work. Yu-Qing Wang and Xing-Jian Chu are the common first authors of the paper. All authors gratefully acknowledge the anonymous reviewers for their valuable comments and suggestions.

References

1. D. C. Ao, R. Jiang, M. B. Hu, Z. Y. Gao and B. Jia, *IEEE Trans. Intell. Transp. Syst.* **1** (2014) 1135.
2. H. J. Ma and Y. M. Jia, *J. Math. Anal. Appl.* **435** (2016) 593.
3. F. Tramontana *et al.*, *Nonlinear Anal., Real World Appl.* **26** (2015) 150.
4. X. Y. Zhou, X. Y. Shi and H. D. Cheng, *Comput. Appl. Math.* **32** (2013) 245.
5. M. Lippi, M. Bertini and P. Frasconi, *IEEE Trans. Intell. Transp. Syst.* **14** (2013) 871.
6. X. Z. Meng, *Appl. Math. Comput.* **217** (2010) 506.
7. T. H. Zhang, T. Q. Zhang and X. Z. Meng, *Appl. Math. Lett.* **68** (2017) 1.
8. X. L. Zhuo and F. X. Zhang, *Qual. Theor. Dyn. Syst.* **1** (2017) 1.
9. Y. Shiomi, T. Taniguchi, N. Uno, H. Shimamoto and T. Nakamura, *Transport. Res. C-Emerg.* **59** (2015) 198.
10. A. Spiliopoulou *et al.*, *Oper. Res.* **17** (2017) 145.
11. X. Z. Meng, S. N. Zhao and W. Y. Zhang, *Appl. Math. Comput.* **266** (2015) 946.
12. X. Meng, R. Liu and T. Zhang, *Nonlinear Anal., Real World Appl.* **16** (2014) 202.
13. B. Q. Guo, H. F. Wang and S. Q. An, *IEEE Trans. Microw. Theory Tech.* **62** (2014) 2084.
14. B. Q. Guo and X. L. Li, *IEEE Microw. Wirel. Compon. Lett.* **23** (2013).
15. B. Q. Guo and G. Wen, *Prog. Electromagn. Res.* **117** (2011) 283.
16. B. Q. Guo, G. J. Wen and S. Q. An, *IET Electron. Lett.* **50** (2014) 149.
17. R. Jiang *et al.*, *Transport. Res. C-Emerg.* **69** (2016) 527.
18. Y. Q. Wang *et al.*, *Comput. Phys. Commun.* **185** (2014) 2823.
19. Y. Q. Wang *et al.*, *Mod. Phys. Lett. B*, doi:10.1142/S021798491750244X (2017) 1750244.
20. Y. Q. Wang *et al.*, *Nonlinear Dynam.* **88** (2017) 2051.
21. M. J. Lighthill and G. B. Whitham, *Proc. R. Soc. Lond. A* **229** (1955) 317.
22. H. J. Payne, Models of freeway traffic and control, in *Mathematical Models of Public Systems*, ed. G. A. Bekey (1971).
23. B. S. Kerner and P. Konhauser, *Phys. Rev. E* **48** (1993) R2335.
24. T. Q. Tang, H. J. Huang, S. C. Wong and R. Jiang, *Chin. Phys. B* **18** (2009) 975.
25. T. Q. Tang, H. J. Huang and H. Y. Shang, *Transp. Res. D: Transp. Environ.* **41** (2015) 423.

26. T. Q. Tang, Z. Y. Yi and Q. F. Lin, *Physica A* **469** (2017) 200.
27. T. Q. Tang, Q. Yu and K. Liu, *Physica A* **466** (2017) 1.
28. T. Q. Tang *et al.*, *J. Adv. Transport.* **48** (2014) 304.
29. S. Xiao and J. Y. Bai, *Mod. Phys. Lett. B* **27** (2013) 1350062.
30. S. Xiao, M. Z. Liu and J. Shang, *Mod. Phys. Lett. B* **26** (2012) 1150036.
31. S. Xiao, J. J. Cai, F. Liu and M. Z. Liu, *Int. J. Mod. Phys. B* **24** (2010) 5539.
32. Y. Liu *et al.*, *Renew. Sust. Energ. Rev.* **62** (2016) 815.
33. S. Xiao, X. Chen and Y. Liu, *Int. J. Mod. Phys. B* **30** (2016) 1650083.
34. S. Xiao *et al.*, *Int. J. Theor. Phys.* **55** (2016) 1642.
35. Y. Q. Wang *et al.*, *Mod. Phys. Lett. B* **28** (2014) 1450123.
36. Y. Q. Wang *et al.*, *Mod. Phys. Lett. B* **31** (2017) 1750104.
37. Y. Q. Wang *et al.*, *Mod. Phys. Lett. B* **28** (2014) 1450064.
38. Y. Q. Wang *et al.*, *Sci. Rep.* **4** (2014) 5459.
39. R. Jiang *et al.*, *Phys. Rev. E* **87** (2013) 012107.
40. L. A. Pipes, *J. Appl. Phys.* **24** (1953) 274.
41. T. Nagatani, *Physica A* **265** (1999) 297.
42. R. Jiang, Q. S. Wu and Z. J. Zhu, *Transport. Res. B* **36** (2002) 405.
43. M. Bando *et al.*, *Phys. Rev. E* **51** (1995) 1035.
44. M. Treiber, A. Hennecke and M. Helbing, *Phys. Rev. E* **59** (1999) 239.
45. R. Jiang *et al.*, *Transp. Res. Proc.* **23** (2017) 157.
46. T. Q. Tang *et al.*, *Physica A* **437** (2015) 55.
47. G. B. Whitham, *Linear and Nonlinear Waves* (Wiley, New York, 1974).